LOCAL ADAPTIVE BIVARIATE SHRINKAGE WITH REDUCED SENSITIVITY

Alexandru Isar[1], IEEE Member, Sorin Moga[2], IEEE Member, Ioan Nafornita[1], IEEE Member, Jean-Marie Augustin[3], Ronan Fablet[3], Xavier Lurton[3] and Dorina Isar[1].

1 University POLITEHNICA
2 Bd. V. Parvan,
1900 Timisoara, Romania
{alexandru.isar}{ioan.nafornita}{dorina.isar}@etc.upt.ro
2 GET - ENST Bretagne
Technopôle de Brest Iroise, CS 83818,
29238 BREST Cedex, France
sorin.moga@enst-bretagne.fr
3 IFREMER - Centre de Brest
Service Acoustique et Sismique (TMSI/AS)
BP 70 Plouzané 29280 France
{augustin}{fablet}{lurton}@ifremer.fr

ABSTRACT

The performance of image denoising algorithms using the Double Tree Complex Wavelet Transform, DTCWT, followed by a local adaptive bishrink filter can be improved by reducing the sensitivity of that filter with the local marginal variance of the wavelet coefficients. In this paper is proposed a solution for the sensitivity reduction based on enhanced diversity. The solution proposed in this paper will be used for the denoising of SONAR images and will be included into the soft SONARSCOPE, in construction at IFREMER-Brest and in evaluation at ENST-Bretagne and "Politehnica" University Timisoara.

1. INTRODUCTION

Some recent research has addressed the development of statistical models of wavelet coefficients of natural images and application of these models to image denoising. Recently highly effective yet simple schemes mostly based on soft thresholding have been developed [1, 2, 10]. In [10], the wavelet coefficients are modelled with a Gaussian apriori density, and locally adaptive estimation is done for coefficients variances. In [1], the inter-scale dependencies are used to improve the performance. The models, which exploit the dependency between coefficients, give better results compared to the ones using an independence assumption [5,8,13,14]. In [3], the wavelet coefficients are modelled with a bivariate Laplace apriori density that takes into account the inter-scale dependencies and locally adaptive estimation is done for coefficient variances. In [4] a similar technique is used but the bivariate apriori density of coefficients is considered of SαS type. This paper presents a new denoising algorithm with improved performance in the uniform zones. It tries to reduce the sensitivity of the local adaptive bishrink filter, [3], in uniform zones. The performance of the new denoising algorithm will be demonstrated and some comparisons with the best available wavelet based image denoising results will be given in order to illustrate the effectiveness of the system.

2. LOCAL ADAPTIVE BISHRINK FILTER

In this paper, the denoising of an image s corrupted by additive white Gaussian noise, AWGN, with variance σ_n^2 will be considered. Let w_{2k} represent the parent of w_{1k}. The problem is formulated in wavelet domain as $y_{1k} = w_{1k} + n_{1k}$ and $y_{2k} = w_{2k} + n_{2k}$ to take into account the statistical dependencies between a coefficient and its parent. We can write:

$$\mathbf{y}_k = \mathbf{w}_k + \mathbf{n}_k. \tag{1}$$

where $\mathbf{w}_k = (w_{1k}, w_{2k})$, $\mathbf{y}_k = (y_{1k}, y_{2k})$ and $\mathbf{n}_k = (n_{1k}, n_{2k})$. In [3], the MAP estimator of w_1 is derived to be:

$$\widehat{w}_1 = \frac{\left(\sqrt{y_1^2 + y_2^2} - \frac{\sqrt{3}\sigma_n^2}{\sigma}\right)_+}{\sqrt{y_1^2 + y_2^2}} \cdot y_1. \tag{2}$$

Here $(g)_+$ is defined as:

$$(g)_+ = \begin{cases} 0, & if\ g < 0 \\ g, & \text{otherwise} \end{cases}. \tag{3}$$

This estimator, named bishrink filter, requires the prior knowledge of the noise variance σ_n^2, and the marginal variance σ^2, for each wavelet coefficient. To estimate the noise variance σ_n^2 from the noisy wavelet coefficients, a robust median estimator is used from the finest scale wavelet coefficients [6]:

$$\hat{\sigma}_n^2 = \frac{\text{median}\left(|y_i|\right)}{0.6745}, \quad y_i \in \text{subband HH}. \tag{4}$$

In [3], the marginal variance of the *k*'th coefficient is estimated using neighboring coefficients in the region *N(k)*, a squared shaped window centered at the *k*'th coefficient with window size 7x7. To make this estimation one gets $\sigma_y^2 = \sigma^2 + \sigma_n^2$, where σ_y^2 is the marginal variance of noisy observations, y_1 and y_2. For the estimation of σ_y^2, in [3] is proposed the following relation:

$$\hat{\sigma}_y^2 = \frac{1}{M} \sum_{y_i \in N(k)} y_i^2, \tag{5}$$

where *M* is the size of the neighborhood *N(k)*. Then σ can be estimated as:

$$\hat{\sigma} = \sqrt{\left(\hat{\sigma}_y^2 - \hat{\sigma}_n^2\right)_+}. \tag{6}$$

The estimator described by (2), (4) and (6) is named local adaptive bishrink filter. One of the most important parameters of the local adaptive bishrink filter is the marginal variance σ. The sensitivity of the estimation $\hat{w}_1$ with $\hat{\sigma}$ is defined by:

$$S_{\hat{w}_1}^{\hat{\sigma}} = \frac{d\hat{w}_1}{d\hat{\sigma}} \cdot \frac{\hat{\sigma}}{\hat{w}_1}. \tag{7}$$

For the coefficients satisfying:

$$\sqrt{y_1^2 + y_2^2} > \frac{\sqrt{3}\hat{\sigma}_n^2}{\hat{\sigma}}, \tag{8}$$

this sensitivity becomes:

$$S_{\hat{w}_1}^{\hat{\sigma}} = \frac{\sqrt{3}\hat{\sigma}_n^2}{\hat{\sigma}\sqrt{y_1^2 + y_2^2} - \sqrt{3}\hat{\sigma}_n^2}.$$

Because the sensitivity is inverse proportional with the marginal variance, the poorer filtering results are obtained in the homogeneous regions of the image.

3. A NEW DENOISING SYSTEM

The details of an image are located in its contours and textures. The corresponding pixels have high or medium local standard deviations. The pixels corresponding to the uniform zones have small local standard deviations. The uniform zones of the image *s* produce wavelet coefficients with small $\hat{\sigma}$, its textures give wavelet coefficients with medium local standard deviations and its contours generate wavelet coefficients with high $\hat{\sigma}$. The perturbation of the uniform zones of the image *s* produced by noise corresponds to the modifications of the wavelet coefficients with small $\hat{\sigma}$, where the sensitivity of the local adaptive bishrink filter is too high. The effect is an important distortion of the uniform zones in the image $\hat{s}$. The goal of this paper is to reduce the distortion of the uniform zones of the image produced by a denoising system based on the DTCWT and the local adaptive bishrink filter. The solution proposed is the enhancement of the estimation diversity. Two types of DTCWT are computed. For each wavelet coefficient with small $\hat{\sigma}$ three variants of bishrink filter are applied obtaining six different estimations $\hat{w}_1$. Averaging these values, a better estimation is obtained. For the wavelet coefficients with higher $\hat{\sigma}$ a reduced number of variants is applied. This procedure is equivalent with the use of six different denoising systems and the fusion of their results. The architecture of the proposed denoising system is presented in figure 1. Two types of wavelet transform DTCWT_A and DTCWT_F are computed obtaining the coefficients w_A and w_F. Three types of filters (similar with the local adaptive bishrink filter) F_1, F_2 and F_3 are used after each DTCWT. Six estimates of the wavelet coefficients $\hat{w}_{1A}$, $\hat{w}_{2A}$, $\hat{w}_{3A}$, $\hat{w}_{1F}$, $\hat{w}_{2F}$ and $\hat{w}_{3F}$ are produced. For each one the IDTCWT is computed, obtaining six estimates, $\hat{s}_{1A}$, $\hat{s}_{2A}$, $\hat{s}_{3A}$, $\hat{s}_{1F}$, $\hat{s}_{2F}$ and $\hat{s}_{3F}$. The image $\hat{s}_{2A}$ is segmented in six classes following the values of the local standard deviations of its pixels. Using the class selectors CS1 − CS6 each image $\hat{s}_{1A}$ - $\hat{s}_{3F}$ is treated in a different manner. The segmentation block, Segm, creates the map of each class (the list of pixels positions belonging to that class). The corresponding class selector, CS, uses each map. These systems pick up the pixels of their input images with the positions belonging to the corresponding map, generating the class of those images. CS1 has only one input and generates the first class of the image $\hat{s}_{2A}$. CS2 has two inputs and generates the second class of the images $\hat{s}_{2A}$ and $\hat{s}_{3A}$ and so on.

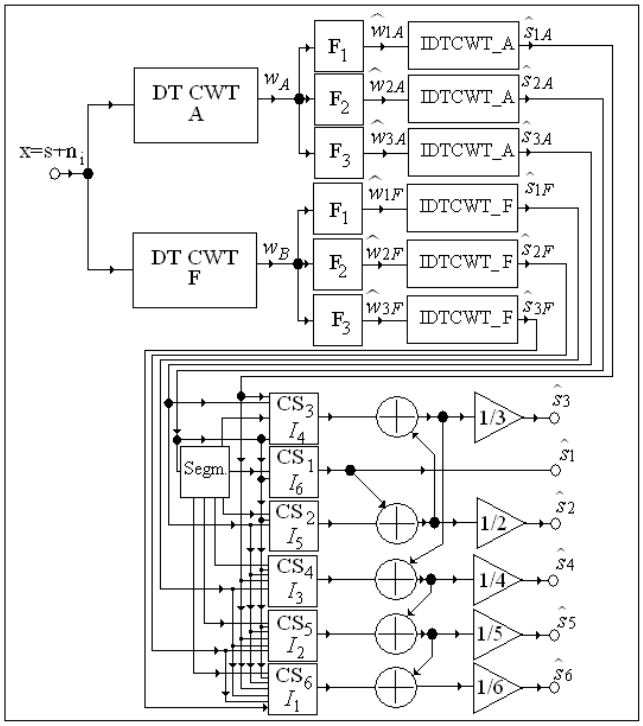

Figure 1. The architecture of the proposed denoising system.

The first class of the final estimate $\hat{s}_1$ is identical with the first class of the image $\hat{s}_{2A}$. The second class of the final result, $\hat{s}_2$ is obtained averaging the pixels belonging to the second class of the images $\hat{s}_{2A}$ and $\hat{s}_{3A}$ and so on. For the last class of the final result, $\hat{s}_6$, containing uniform zones, all the pixels belonging to the sixth class of the estimates, $\hat{s}_{1A}$, $\hat{s}_{2A}$, $\hat{s}_{3A}$, $\hat{s}_{1F}$, $\hat{s}_{2F}$ and $\hat{s}_{3F}$ are averaged.

3.1. BISHRINK FILTER VARIANTS

In the following are presented the three proposed variants F_1, F_2 and F_3. The last two variants correspond to two diversification principles: the estimation of the local standard deviations of the wavelet coefficients and the pdf of those coefficients. Another diversification principle is also used: the construction of the DTCWT. These diversification principles are described in the following.

3.1.1. CONSTRUCTION OF THE DTCWT

There are two kinds of filters used for the computation of the DTCWT: for the first level and for the other levels, [5]. The diversification is realized by the selection of two types of filters for the first level. The first one is selected from the (9,7)-tap Antonini filters pair and the second one corresponds to the pair of Farras nearly symmetric filters for orthogonal 2-channel perfect reconstruction filter bank, [6]. The filter F1 is a local adaptive bishrink filter.

3.1.2. ESTIMATION OF LOCAL VARIANCES

The estimation of σ in (6) is not very precise for two reasons. First, it is based on the correct assumption that y_1 and y_2 are modelled as zero mean random variables. But their restrictions to the finite neighbourhood *N (k)* are not necessary zero mean random variables. So, is better to first estimate the means in the neighbourhood:

$$\hat{\mu}_y = \frac{1}{M} \sum_{y_i \in N(k)} y_i, \tag{10}$$

and then their variances:

$$\hat{\sigma}_y^2 = \frac{1}{M} \sum_{y_i \in N(k)} \left(y_i - \hat{\mu}_y \right)^2, \tag{11}$$

Finally, the relation (6) can be applied. The second reason of imprecision is the fact that relation (6) refers only to one of the two trees of the DTCWT. In the following the detail wavelet coefficients produced by this three will be indexed with *re*. The detail wavelet coefficients produced by the other tree will be indexed with *im*. Applying in order the relations (10), (11) and (6) for the two trees implementing each of the DTCWT, the local parameters ${}_{re}\hat{\mu}_y$, ${}_{re}\hat{\sigma}_y^2$, ${}_{re}\hat{\sigma}$, ${}_{im}\hat{\mu}_y$, ${}_{im}\hat{\sigma}_y^2$ and ${}_{im}\hat{\sigma}$ are computed in each neighbourhood *N (k)*. Then the global estimation of the marginal standard deviation can be done:

$$\hat{\sigma} = \frac{{}_{re}\hat{\sigma} + {}_{im}\hat{\sigma}}{2} \tag{12}$$

The filter F2 is a variant of the bishrink filter based on this estimation of the marginal standard deviation.

3.1.3. PDF OF WAVELET COEFFICIENTS

The 2D DWT is built with separable orthogonal mother wavelets, having a given regularity. At each DWT's iteration, the lines of the input image (obtained at the end of the previous iteration) are low-pass filtered with a filter having the impulse response m_0 and high-pass filtered with the filter m_1. Then the lines of the two images obtained at the output of the two filters are decimated with a factor of 2. Next, the columns of the two images obtained are low-pass filtered with m_0 and high-pass filtered with m_1. The columns of those four images are also decimated with a factor of 2. Four new sub-images (representing the result of the current iteration) are generated. The first one, obtained after two low-pass filtering, is named approximation sub-image (or LL image). The others three are named detail sub-images: LH, HL and HH. The LL image represents the input for the next iteration. In the following, the coefficients of the DWT will be noted with ${}_x w_m^o$, where *x* represents the image who's DWT is computed, *m* represents the iteration index (the resolution level) and *o* = 1, for the HH image, *o* = 2, for the HL image, *o* = 3, for the LH image and *o* = 4, for the LL image. These coefficients are computed using the following relation:

$${}_x w_m^o[b,c] = \left\langle x(\tau_1,\tau_2), \psi_{m,b,c}^o(\tau_1,\tau_2) \right\rangle, \tag{13}$$

where the wavelets can be factorised:

$$\psi_{m,b,c}^o(\tau_1,\tau_2) = \alpha_{m,b,c}^o(\tau_1) \cdot \beta_{m,b,c}^o(\tau_2), \tag{14}$$

and the two factors can be computed using the scale function φ(τ) and the mother wavelets ψ (τ) with the aid of the following relations:

$$\alpha_{m,b,c}^o(\tau) = \begin{cases} \varphi_{m,b}(\tau), & o = 1,4 \\ \psi_{m,b}(\tau), & o = 2,3 \end{cases}, \tag{15}$$

$$\beta_{m,b,c}^o(\tau) = \begin{cases} \varphi_{m,b}(\tau), & o = 2,4 \\ \psi_{m,b}(\tau), & o = 1,3 \end{cases}, \tag{16}$$

where:

$$\varphi_{m,b}(\tau) = 2^{-\frac{m}{2}} \varphi\left(2^{-m}\tau - b\right), \tag{17}$$

$$\psi_{m,b}(\tau) = 2^{-\frac{m}{2}} \psi\left(2^{-m}\tau - b\right). \tag{18}$$

Each sub-image has its own pdf. The pdfs computation is based on the relation between the pdfs of the random variables, from the input and the output of a digital filter. This is a sequence of convolutions which number is equal with the number of the filter coefficients. The pdfs of the wavelet coefficients, ${}_x w_m^o$, can be expressed with the aid of the pdf of the input image, *x*, using the relation, [7]:

$$f_{x w_m^o}(a) = \underset{i_1=1}{\overset{M(o)N(o)}{*}} \underset{j_1=1}{\overset{M_0}{*}} \underset{i_2=1}{\overset{M_0}{*}} \underset{j_2=1}{\overset{M_0}{*}} \ldots \underset{i_v=1}{\overset{M_0}{*}} \underset{j_v=1}{\overset{M_0}{*}} f_d(o,i_1,j_1,i_2,j_2,\ldots,i_v,j_v,a), \quad (19)$$

where:

$$f_d(o,i_1,\ldots,j_v,a) = G(o,i_1,\ldots,j_v) \; f_x\left(G(o,i_1,\ldots,j_v)a\right), \quad (20)$$

and :

$$G(o,i_1,\ldots,j_v) = \frac{1}{F(o,i_1,j_1)\prod_{h=2}^{v} m_0[i_h]m_0[j_h]}, \quad (21)$$

where:

$$F(o,i_1,j_1) = \begin{cases} m_0[i_1]m_0[j_1], & for \quad o=4 \\ m_0[i_1]m_1[j_1], & for \quad o=3 \\ m_1[i_1]m_0[j_1], & for \quad o=2 \\ m_1[i_1]m_1[j_1], & for \quad o=1 \end{cases}. \quad (22)$$

M_0 represents the length of the impulse response m_0, M_1 the length of m_1 and the numbers of the first two groups of convolutions in relation (19) are given by the relation:

$$M(o) = \begin{cases} M_0, & for \quad o=4 \\ M_0, & for \quad o=3 \\ M_1, & for \quad o=2 \\ M_1, & for \quad o=1 \end{cases} \quad and \quad N(o) = \begin{cases} M_0, & for \quad o=4 \\ M_1, & for \quad o=3 \\ M_0, & for \quad o=2 \\ M_1, & for \quad o=1 \end{cases}. \quad (23)$$

In conformity with (19), each pdf of the wavelet coefficients is a sequence of convolutions. Hence, the random variable representing the wavelet coefficients can be written like a sum of independent random variables. So, the central limit theorem can be applied. This is the reason why the pdf of the wavelet coefficients tends asymptotically to a Gaussian, when the number of convolutions in (19) (the DWT iterations number) tends to infinity. This number depends on the mother wavelets used and on the number of iterations of the DWT. For mother wavelets with a long support, this number becomes large very fast (for a small number of iterations). After three iterations of each Discrete Wavelet Transform, DWT, representing one tree of a DTCWT, the pdf of wavelet coefficients can be considered Gaussian. For the first three iterations, heavy-tailed models must be considered. In [7] is proposed a new variant of local adaptive bishrink filter. This system, named mixed bishrink filter, acts for the first three iterations of each DWT like a local adaptive bishrink filter (the pdf of the wavelet coefficients is considered of Laplace type). For the forth iteration it acts like a local adaptive Wiener filter and for the fifth iteration of each DWT (the last one) it acts like a hard thresholding filter with the threshold equal with $3\hat{\sigma}_n$ (the pdf of the wavelet coefficients is considered Gaussian). The MAP estimation of $\boldsymbol{w}$, realized using the observation $\boldsymbol{y}$, is given by, [3]:

$$\hat{w}(y) = \underset{w}{arg\,max}\left\{ln\left(f_n(y\text{-}w)f_w(w)\right)\right\} \quad (24)$$

where $f_{\mathbf{x}}$ represents the pdf of the vector $\boldsymbol{x}$. The solution of the problem in last relation is described in (2) and (3) for the case of the bishrink filter. This solution is obtained considering a Laplace model for $f_{\mathbf{w}}$ and a Gaussian model for $f_{\mathbf{n}}$. It corresponds to the mixed bishrink filter for the first three iterations of the DTCWT. The solution of the problem in last relation obtained considering that both $f_{\mathbf{w}}$ and $f_{\mathbf{n}}$ are Gaussians is the zero order Wiener filter, described by the input-output relation:

$$\hat{w}_1 = \frac{\sigma^2}{\sigma^2 + \sigma_n^2} y_1 \quad (25)$$

It corresponds to the mixed bishrink filter for the forth iteration of the DTCWT. Finally, for the last iteration of the DTCWT the mixed bishrink filter corresponds to a hard thresholding filter. The mixed bishrink filter is named F3.

3.2. CLASSIFICATION

The image $\hat{s}_{2A}$ is segmented in classes whose elements have a value of the local variance, $\hat{\sigma}_{2A}$, belonging to one of six possible intervals $I_p = \left(\alpha_p \hat{\sigma}_{2A\,max}, \alpha_{p+1}\hat{\sigma}_{2A\,max}\right)_{p=\overline{1,6}}$, where:

$$\alpha_1 = 0, \quad and \quad \alpha_7 = 1. \quad (26)$$

The class selector CS_p in figure 1, selects the class associated to the interval I_{7-p}. For uniform regions $\hat{\sigma}$ is proportional with $\hat{\sigma}_{2A}$. Preliminary tests proved that the six estimates are classified from better to poor in the following sequence: $\hat{s}_{2A}$, $\hat{s}_{3A}$, $\hat{s}_{1A}$, $\hat{s}_{1F}$, $\hat{s}_{2F}$ and $\hat{s}_{3F}$, from the pick signal to noise ratio, PSNR, point of view. These tests also suggest the following values for the bounds of the intervals I_p: $\alpha_2 = 0.025$, $\alpha_3 = 0.05$, $\alpha_4 = 0.075$, $\alpha_5 = 0.1$, $\alpha_6 = 0.25$. In the following figures is presented such a segmentation experiment. The original image, Barbara, is presented in figure 2, and the images corresponding to the six classes already mentioned are represented in figures 3-8. The pixels not belonging to a specified class are represented in black. In figure 3 is represented the image corresponding to the last class, containing the pixels with the higher local variances. In figures 4, 5, 6 and 7 are represented the images corresponding to intermediate classes, containing pixels with reduced local variances and in figure 8 is represented the image corresponding to the first class, containing the pixels with the smaller local variances.

Figure 2. Original image.

Figure 3. The class corresponding to interval I_6. It contains the largest contours.

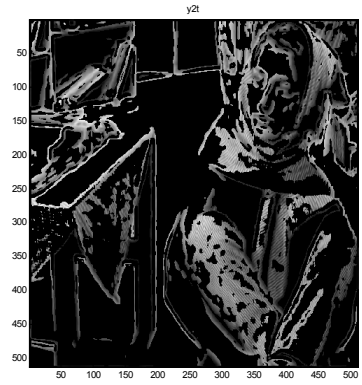

Figure 4. The class corresponding to interval I_5. It contains contours and textures.

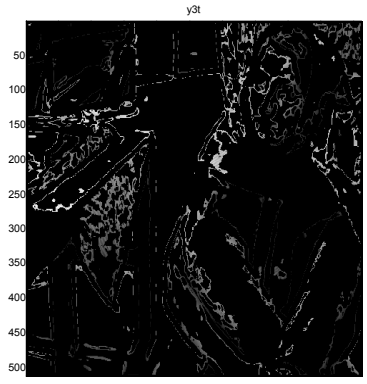

Figure 5. The class corresponding to interval I_4. It contains contours and textures.

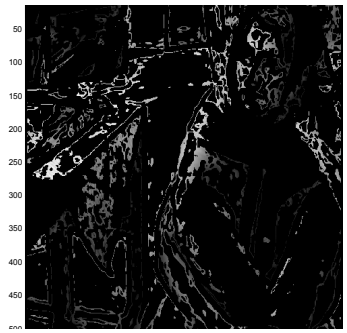

Figure 6. The class corresponding to interval I_3.

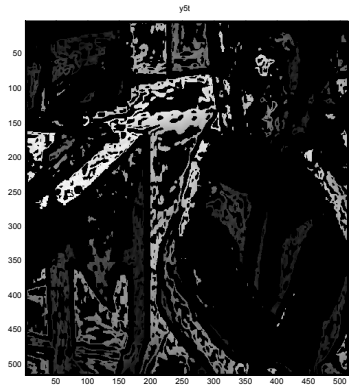

Figure 7. The class corresponding to interval I_2. It contains textures.

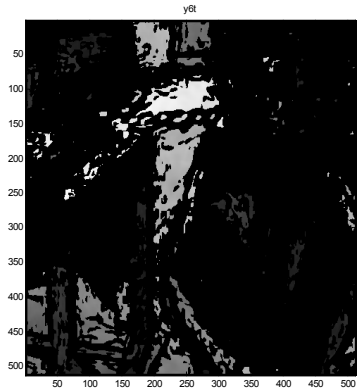

Figure 8. The class corresponding to interval I_1. It contains homogenous regions.

3.3. FUSION

The first class of the final result contains some pixels of the image $\hat{s}_{2A}$. The second class of the final result is obtained by the fusion of the second classes of two partial results, $\hat{s}_{2A}$ and $\hat{s}_{3A}$ and so on. The sixth class of the final result is obtained by the fusion of the sixth classes of all the partial results, $\hat{s}_{2A}$, $\hat{s}_{3A}$, $\hat{s}_{1A}$, $\hat{s}_{1F}$, $\hat{s}_{2F}$ and $\hat{s}_{3F}$. These fusions are realized by averaging. In the following is explained why

the averaging was preferred for fusion. The fusion of the p'th class of the final result can be done with the following relation:

$$\widehat{X}_p = \sum_{l=1}^{p} \beta_l X_l, \tag{27}$$

where X_l represent the l'th class of the partial results involved. The coefficients β_l are constrained to satisfy the perfect reconstruction condition:

$$\sum_{l=1}^{p} \beta_l = 1. \tag{28}$$

These coefficients are selected to minimize the mean square error between the useful component of the input image X and $\widehat{X}_p$. This error has the expression:

$$MSE = E\left\{\left(\widehat{X}_p - X\right)^2\right\} = \sigma_X^2 - 2E\left\{XX_p\right\} + \sigma_{\widehat{X}_p}^2. \tag{29}$$

This minimization can be done using the Lagrange multipliers method. The associated functional has the expression:

$$F\left(\beta_1, \beta_2, ..., \beta_p\right) = \sigma_X^2 - 2E\left\{XX_p\right\} + \sigma_{\widehat{X}_p}^2 - \lambda\left(\sum_{l=1}^{p} \beta_l - 1\right). \tag{30}$$

The minimization condition is:

$$\frac{\partial F}{\partial \beta_e} = 0, \tag{31}$$

equivalent with:

$$-2E\left\{XX_e\right\} + 2E\left\{\left(\sum_{l=1}^{p} \beta_l X_l\right) X_e\right\} - \lambda = 0. \tag{32}$$

Using the notations:

$$E\left\{XX_e\right\} = i_e \text{ and } \mathrm{E}\left\{\mathrm{X}_1 X_e\right\} = c_{l,e}, \tag{33}$$

the last relation becomes:

$$\sum_{l=1}^{p} \beta_l \cdot c_{l,e} = \frac{\lambda}{2} + i_e, \quad \mathrm{e}=\overline{1,\mathrm{p}}. \tag{34}$$

The partial results, X_l, are estimations of the same useful image, X, obtained using a denoising method based on the DTCWT and a variant of bishrink filter. Because the noise in the DWT domain is white and Gaussian, it can be supposed that the partial results are of the form:

$$X_l = X + \xi_l, \quad l = \overline{1, p}. \tag{35}$$

where ξ_l represent p realizations of a white Gaussian noise. This is the reason why it can be written:

$$i_e = \sigma_X^2, \ \mathrm{c}_{\mathrm{l,e}} = \begin{cases} \sigma_X^2 + \sigma_\xi^2, & \text{for } l = e \\ \sigma_{\mathrm{X}}^2, & \text{in rest} \end{cases}, \tag{36}$$

and the relation (34) becomes the following system of equations:

$$\begin{cases} \beta_1\left(\sigma_X^2 + \sigma_\xi^2\right) + \beta_2\sigma_X^2 + ... + \beta_p\sigma_X^2 = \dfrac{\lambda}{2} + \sigma_X^2 \\ \beta_1\sigma_X^2 + \beta_2\left(\sigma_X^2 + \sigma_\xi^2\right) + ... + \beta_p\sigma_X^2 = \dfrac{\lambda}{2} + \sigma_X^2 \\ \quad . \qquad\qquad\qquad\qquad . \\ \quad . \\ \quad . \\ \beta_1\sigma_X^2 + \beta_2\left(\sigma_X^2 + \sigma_\xi^2\right) + ... + \beta_p\sigma_X^2 = \dfrac{\lambda}{2} + \sigma_X^2 \end{cases} \tag{37}$$

Using the constraint from (24), the last system of equations takes the simplified form:

$$\sigma_X^2 + \beta_e\sigma_\xi^2 = \frac{\lambda}{2} + \sigma_X^2, \quad e = \overline{1, p}, \tag{38}$$

with the solutions:

$$\beta_1 = \beta_2 = ... = \beta_p = \frac{\lambda}{2\sigma_\xi^2}, \tag{39}$$

Taking into account once more the constraint (28) the solutions become:

$$\beta_1 = \beta_2 = ... = \beta_p = \frac{1}{p}. \tag{40}$$

So, the best synthesis solution for the minimization of the approximation mean square error is the averager.

The uniform zones treatment can be completed by some final adjustments. The results corresponding to the intervals $I_1 \div I_3$, $\hat{s}_6 \div \hat{s}_4$, contain the uniform zones. The most uniform regions are found in the image that corresponds to the interval I_1. The final adjustments suppose the mean filtering of the results corresponding to the intervals $I_1 \div I_3$, using decreasing windowsizes: 7x7 for $\hat{s}_6$, 5x5 for $\hat{s}_5$ and 3x3 for $\hat{s}_4$. These final adjustments are applied only if the PSNR of the noisy image is inferior to 20 dB.

4. RESULTS

We compared the proposed algorithm to other effective systems in the literature, namely the local adaptive bishrink filter in [3], the denoising system based on the steerable pyramid proposed in [8] and the denoising processor introduced in [4]. The comparison was done using for images: Peppers, Lena, Boats and Barbara, all having the same size, 512x512 pixels. Let s and $\hat{s}$ denote the original and the denoised image. The rms error is given by:

$$\varepsilon = \sqrt{\frac{1}{N}\sum_q \left(s_q - \hat{s}_q\right)^2} \tag{41}$$

where N is the number of pixels. The PSNR in dB is given by:

$$PSNR = 20 \cdot log_{10}\left(\frac{256}{\varepsilon}\right) \tag{42}$$

One example for the image Peppers is presented in figure 8.

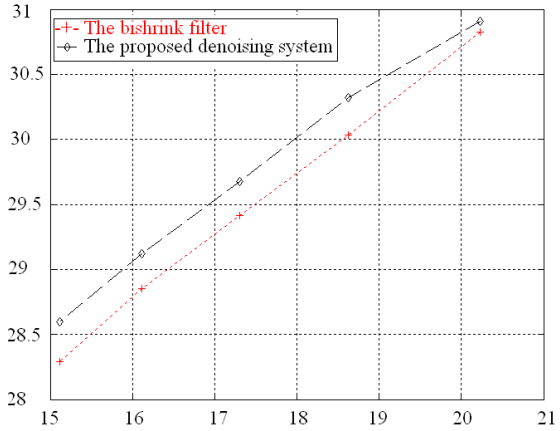

Figure 8. A comparison of the dependencies of the output PSNR on the input PSNR for the bishrink filter and the proposed denoising system for the image Peppers.

The dependencies between the output and the input PSNRs for the proposed denoising system and for the local adaptive bishrink filter are compared for five values of σ_n: 25, 30, 35, 40 and 45. One example for the image Lena is given in figure 9. The original image was perturbed with an AWGN with $\sigma_n = 100$. A region obtained cropping the image $\hat{s}_{2A}$ is illustrated in figure 9 a). The same region was also extracted from the image $\hat{s}$ and is illustrated in figure 9 b). The proposed system decreases the distortions in the uniform zones.

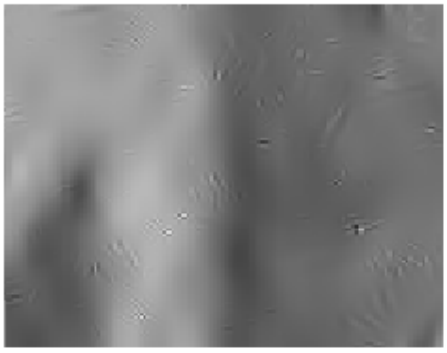

a)

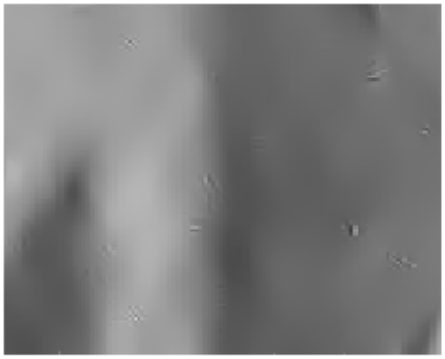

b)

Figure 9. A comparison of the treatments of uniform zones realized by the bishrink filter a) and the proposed denoising system b), for a zoomed portion of image Lena.

The PSNR values of the denoising systems already mentioned at the beginning of this paragraph are tabulated in Table 1. The comparisons already presented take into account only the PSNR, a global quality measure. But the local adaptive bishrink filter and the proposed denoising system make different treatments of different regions. We also compared these two denoising systems from the uniform zones treatment point of view.

Table 1

The PSNR values of denoised images for different test images and noise levels (σ_n) of (A) noisy, (B) denoising system in [8], (C) denoising processor in [4] with (+) or without (-) local estimation (l.e.), (D) local adaptive bishrink filter in [3] and (E) proposed algorithm.

σ_n	A	B	C	D	E
Lena			- l.e.		
10	28.18	35.31	34.75	35.34	35.36
15	24.65	33.55	33.03	33.67	33.68
20	22.14	32.31	31.87	32.40	32.43
25	20.17	31.33	30.89	31.40	31.49
30	18.62	-	30.18	30.54	30.83
Boats		-	+l.e.		
10	28.16	-	33.09	33.10	33.33
15	24.65	-	31.44	31.36	31.45
20	22.15	-	30.19	30.08	30.14
25	20.15	-	29.21	29.06	29.12
30	18.62	-	28.51	28.31	28.38
Barbara					
10	28.16	33.45	-	33.35	33.78
15	24.63	31.22	-	31.31	31.57
20	22.14	29.71	-	29.80	30.03
25	20.18	28.57	-	28.61	28.88
30	18.62	-	-	27.65	27.93

5. CONCLUSION

This paper presents an effective image-denoising algorithm that optimises the treatment of uniform zones. Our algorithm is inspired from [3], [9], [11], [12] and [14] but the diversity enhancement technique proposed can be used also for the improvement of other denoising systems. In [3] is noted that the Matlab implementation of their algorithm takes 25 seconds for a 512x512 image on a 450 MHz Pentium II. The Matlab program for the proposed algorithm takes 82 seconds for a 512x512 image on a 2.4 GHz Pentium IV.

We presented our results and compared with the other published results in order to illustrate the effectiveness of the proposed algorithm. The comparison suggests the new denoising results are competitive with the best wavelet-based results reported in literature. Some choices rests heuristic in the proposed algorithm:

- the cost functional to be minimized (we have chosen the mean square error, to maximize the output PSNR), but this functional is not optimal from the human visual system point of view;
- the segmentation threshold values, α_k (these values seems to depend on the useful component of the noisy image) and the number of classes used for segmentation (we have chosen a number of six classes because we developed three different filters F_1-F_3);
- the models used for the construction of the different variants of the bishrink filter used in our denoising system.

One of our future research directions suggested by this paper is the formalization of those choices. Another future research direction will be the inclusion of the proposed algorithm into a SONAR images denoising system. The variants of bishrink filter, already mentioned in this paper, were already included into such denoising systems and the results obtained were already reported in [7] and in other reports. Also, these other variants of SONAR images denoising systems were already included in the software SONARSCOPE and are used by the personal of IFREMER Brest. The new SONAR images denoising system will be also included in SONARSCOPE.

Finally, another future direction for this paper is the substitution of the DTCWT with another complex wavelet transform. The new transform will have all the advantages of the DTCWT: reduced redundancy, good translation invariance and good directional selectivity but it will have supplementary another very nice characteristic the facility to enhance its diversity. The conception of this new wavelet transform represents one of the subjects of a PhD thesis advised in common by a professor from ENST-Bretagne and a professor from the Electronics and telecommunications faculty of the Politehnica University Timisoara.

REFERENCES

[1] Z. Cai, T. H. Cheng, C. Lu, and K. R. Subramanian. Efficient wavelet-based image denoising algorithm. Electronics Letters, 37 (11):683-685, May 2001.

[2] S. Chang, B. Yu, and M. Vetterli. Adaptive wavelet thresholding for image denoising and compression. IEEE Trans. on Image Processing, 9 (9):1522-1531, 2000.

[3] L. Sendur and I. W. Selesnick. Bivariate shrinkage with local variance estimation. IEEE Signal Processing Letters, 9 (12):438-441, December 2002.

[4] A. Achim and E. E. Kuruoglu. Image Denoising Using Bivariate α-Stable Distributions in the Complex Wavelet Domain. IEEE Signal Processing Letters, 12(1):17-20, January 2005.

[5] N. Kingsbury. Complex Wavelets for Shift Invariant Analysis and Filtering of Signals. Appl. and Comput. Harmonic Analysis 10:234-253, 2001.

[6] A. Abdelnour and I. W. Selesnick. Nearly symmetric orthogonal wavelet bases. Proc. IEEE Int. Conf. Acoust., Speech, Signal Processing (ICASSP), May 2001.

[7] A. Isar, S. Moga, D. Isar, J. M. Augustin and X. Lurton. Multi-scale MAP Despeckling of SONAR Images. Proceedings of IEEE International Conference Oceans'05, June 2005, Brest, France.

[8] J. Portilla, V. Strela, M. Wainwright and E. Simoncelli. Adaptive Wiener Denoising Using Gaussian Scale Mixture Model. Proc. ICIP, 2001.

[9] S. G. Chang, B. Yu, and M. Vetterli. Spatially adaptive wavelet thresholding with context modelling for image denoising. IEEE Trans. on Image Processing, 9 (9):1522-1531, 2000.

[10] M. K. Mihcak, I. Kozintsev, K. Ramchandran and P. Moulin. Low-complexity image denoising based on statistical modeling of wavelet coefficients. IEEE Signal Processing Letters, 6 (12) : 300-303, 1999.

[11] L. Sendur and I.W. Selesnick. A bivariate shrinkage function for wavelet based denoising. IEEE International Conference on Acoustics, Speech and Signal Processing - ICASSP'02, 2002.

[12] L. Sendur and I. W. Selesnick. Bivariate shrinkage functions for wavelet-based denoising. IEEE Transactions on Signal Processing, 50(11):2744-2756, November 2002.

[13] M. J. Wainwright and E. P. Simoncelli. Scale mixtures of Gaussians and the statistics of natural images. Adv. Neural Information Processing Systems, 12, May 2000.

[14] G. Fan, X. G. Xia. Image denoising using a local contextual hidden Markov model in the wavelet domain. IEEE Signal Processing Letters, 8 (5) : 125-128, May 2001.